Laboratory Report
of
National Metrology Institute of Japan (NMIJ/AIST)
and Japan Electric Meters Inspection Corporation (JEMIC)
2019-2021

At NMIJ/AIST, there are five research groups in the electrical standards area. They are the Applied Electrical Standards Group, the Quantum Electrical Standards Group, the Radio-Frequency Standards Group, the Electromagnetic Fields Standards Group, and the Electromagnetic Measurement Group.

The Applied Electrical Standards Group takes charge of the AC/DC transfer, the impedance and the power standards. The Quantum Electrical Standards Group covers the Josephson voltage and the quantum Hall resistance standards.

The Radio-Frequency Standards Group takes charge of RF power, voltage, noise, and attenuation standards. The Electromagnetic Fields Standards Group covers antenna properties, electric field and magnetic field standards. The Electromagnetic Measurement Group takes charge of RF impedance (S-parameter) standards and material properties.

1. Josephson Voltage

1.1 PJVS and Zener Voltage Standards

A liquid-helium-free PJVS has been utilized since 2015 for calibrations of Zener voltage standards with the CMC values, 8 nV for 1 V and 45 nV for 10 V, same as those for our conventional JVS system cooled with liquid helium. We are now attempting to develop an AC voltage calibration system using PJVS. Development of Zener voltage standards are also now in progress in collaboration with ADC Corporation. We are continuing to investigate the environmental-condition dependences of the voltage outputs of prototype Zener modules. Excelent stability in the nominal 10 V and 7.2 V outputs for temperature, ambient-pressure and relative-humidity changes has been confirmed. (Contact: Michitaka Maruyama, m-maruyama@aist.go.jp).

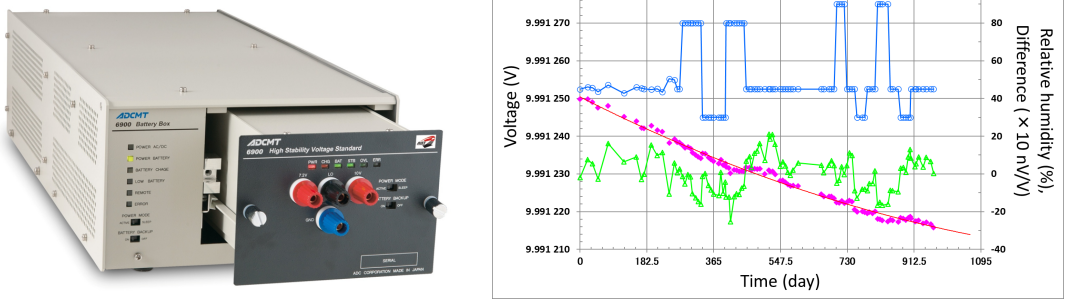

Fig.1 Prototype of a Zener votage standard and its relative-humidity dependence.

1.2 Thermodynamic temperature measurement

We measured the thermodynamic temperature of the melting point of gallium TGa using a Johnson noise thermometer (JNT) with an integrated quantum voltage noise source (IQVNS) as a reference. TGa was calculated using the fundamental constants recommended by the Committee on Data for Science and Technology (CODATA) for the revision of the International System of Units (SI). The measured TGa is consistent with the value defined in the International Temperature Scale of 1990.The power spectral density of output signal of IQVNS has been fixed so far. In order to use IQVNS as a reference for the measurement of thermodynamic temperature at various temperature fixed points, the power spectral density of the output signal of IQVNS should be variable. We improved part of the design of the device to be able to change the power spectral density of the output signal. (Contact: Chiharu Urano, c-urano@aist.go.jp).

2. Resistance

2.1 Standard Resistors

Development of compact and ultra-stable 1 Ω and 1 kΩ standard resistors has been finished, and resistors with 10 kΩ are in progress of evaluation and development. The best resistors display extremely small average drift rates and temperature coefficients, and other performances, e.g.,

- 1 Ω: 4.2 nΩ/(Ω year), 4 nΩ/(Ω ˚C) at 23 ˚C,
- 10 Ω: 0.53 nΩ/(Ω year), 1 nΩ/(Ω ˚C) at 23 ˚C,
- 100 Ω: 50 nΩ/(Ω year), < 20 nΩ/(Ω ˚C) at 23 ˚C, deviation by transportation: < 10 nΩ/Ω, power and humidity coefficients are negligible,
- 1 kΩ: < 10 nΩ/(Ω year), 1.7 nΩ/(Ω ˚C) at 23 ◦C.

(note that the average drift rate and temperature coefficient of each resistance value does not come from the same resistor). It is demonstrated that this excellent performance is

suitable for utilization in national metrology institutes and international comparisons. (Contact: Takehiko Oe, t.oe@aist.go.jp).

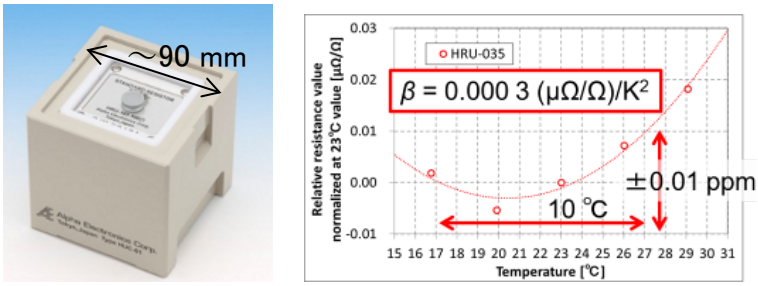

Fig. 2 Picture and temperature-resistance curve of developed 100 Ω standard resistor.

2.2 Qauntized Hall array device

Some 1 MΩ quantum Hall array devices were fabricated and evaluated. The deivces have simple configulation and consist of 88 Hall bars. They have the nominal quantized resistance value of $10^6 \times (1 + 246.289 \times 10^{-6})$ Ω and its quantized value was evaluated using a cryogenic current comparator (CCC) bridge at NIST. The below graph shows the magnetic field dependence of the device. At the center of the plateau, the measurement was repeated some times and the measured value was scattered from –18 nΩ/Ω to +17 nΩ/Ω and the averaged value was +4 μΩ/Ω. The devices showed flat magnetic field dependence for more than 1 T. These evaluation results were presented at CPEM2020. (Contact: Takehiko Oe, t.oe@aist.go.jp).

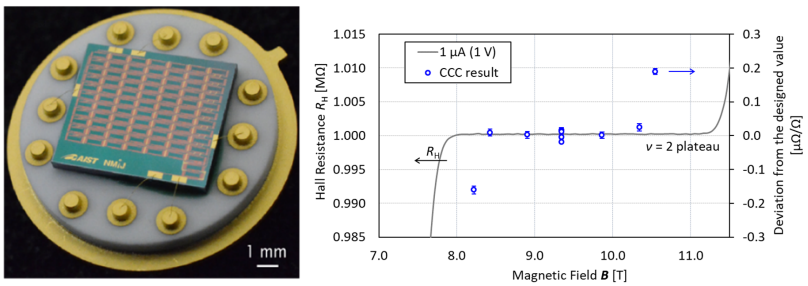

Fig. 3 Picture and the magnetic field dependence of the 1 MΩ array device.

2.3 Contact Resistance Evaluation of Wire Harness

To establish a relationship between the physical structure of electrical contact boundary and contact resistance, NMIJ developed a method for evaluating that using a physical simulated sample created via nanofabrication. Several samples with various distribution of "contact area" were made and their resistances were measured precisely. It was demonstrated experimentally that our result is in good agreement with an expression for constriction resistance.

Impedance measurement was introduced as a degradation diagnosis method for contacts of wire harness by a nondestructive test. It was found that the changes in reactance at a certain frequency behave characteristically and independently of the DC resistance changes during accelerated test. The degradation degree of contacts was estimated by the change in impedance.

3. DC Current (single electron pumping)

Towards a realization of the current standard based on the single-electron pumping, we investigate the physics of low-temperature electron transport phenomena in various types of single-electron devices, i.e. superconductor-insulator-normal- insulator-superconductor (SINIS) turnstiles, gate-confined quantum dots, and graphene- or nanotube-based single-electron transistors.

On SINIS turnstiles, in our early studies, we had discovered the new phenomenon that is a reduction of the single-electron pumping error induced by a weak magnetic field applied to the device. The origin of this phenomenon is related to the suppression of inverse-proximity effect at the interface between superconducting leads and a normal metal island. The inverse proximity effect cause the quasiparticle trap at the interface, namely it leads to the overheating of the junction. The magnetic field weaken the inverse proximity effect and helps to lease the quasiparticle. We justify this scenario from numerical analysis and controlling the tunnel resistance. Aiming at further reducing the pumping error, we extended the research to that based on another pumping mechanism. In one instance, we investigated a GaAs-based gate-defined quantum dot and demonstrated single-parameter pumping. In addition, we developed an air-bridge based parallel integration of this pump to demonstrate a synchronized parallel pumping that can generate a larger current otherwise unattained. In this study, we succeded to operate the GaAs single electron device with sigma-delata madulated pulses for the arbitrary wave generation. This technique is thought to be useful for the calibration of current noise in the shot noise measurement. Also we start to measure the Si single electron pump device in collaboration with NTT group. At present we succeded to operate single electron pumping at 1 GHz with 10^{-6} uncertainty. Now we try to operate this type of device in parallel to generate large (a few nano ampere) current.

These single-electron devices are planned to be integrated with the quantum metrology triangle experiment that combine the single-electron device with the quantum Hall resistance and Josephson voltage standards. Towards this futuristic experiment, we had introduced a dry dilution refrigerator; An ample open space offered by this refrigerator allows us to integrate the whole components required for the triangle experiment

including a cryogenic current comparator into one system. Electric noise filters and high-frequency wiring are now designed and constructed to complete this setup. Also to operate Josephson voltage standard and quantum Hall array device inside the dilution refrigerator, we are installing additional cold stage and try to operate these quantum standards.

4. LF-Impedance

AC resistor calibration service has been kept in the range of 10 Ω up to 100 kΩ at 1 kHz and 10 kHz. Standard capacitor (dry-nitrogen or used silica dielectric) calibration service has been kept in the range of 10 pF up to 1000 pF at 1 kHz, 1.592 kHz. (Contact: Atsushi Domae, domae-atsushi@aist.go.jp).

NMIJ has started a development of precision measuring techniques for diagnosis of the energy storage devices such as lithium-ion batteries and super-capacitors by using an impedance spectroscopy method. We have a plan to establish a metrology for evaluating the storage power devices. Preliminary impedance measurements for lithium-ion battery cells in the range of 10 mHz – 10 kHz demonstrated that the impedance value for unused cells is clearly distinguished from that for used-up cells. Impedance spectra for the unused cells which are obtained under 100 mΩ indicate that the evaluations of the uncertainties should be required for detecting a faint sign or a symptom of degradations of storage devices. We have developed an electrochemical impedance measurement system and have evaluated the type-A uncertainty for the impedance spectra which was estimated to be less than 0.2 mΩ.

AIST established the Global Zero Emission Research Center (GZR) in 2020. GZR has a mission for an international joint research base for zero emission technologies. GZR started to research for innovative environmental and energy technologies, including in the fields of renewable energy, storage batteries, hydrogen, and so on. NMIJ joined in GZR and has started the research of the safety and reliability evaluation method for solid oxide electrochemical cells and lithium ion batteries by using precision impedance and charge-discharge measurements.

(Contact: Norihiko Sakamoto, n-sakamoto@aist.go.jp).

Fig. 4 Photograph of the electrochemical impedance measurement system developed using the Frequency Response Analyzer and the Potentio-Galvano Stat.

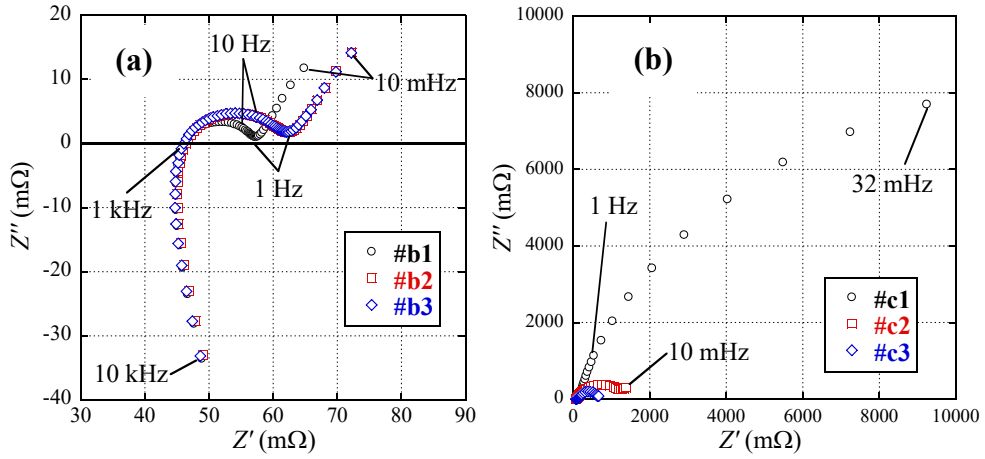

Fig. 5 Nyquist plot of the impedance spectra for the 18650-type lithium-ion batteries: (a) the unused samples and (b) used-up samples. Obvious change in impedance spectra was observed with the progression of the charge/discharge cycle.

5. AC/DC transfer

NMIJ has provided ac-dc voltage difference transfer calibration of thermal converters in the voltage range from 10 mV to 1000 V and in the frequency range from 10 Hz to 1 MHz, and AC voltage calibration below 10 Hz. We have been participating in APMP Comparison for " APMP.EM-K12" of AC/DC current transfer difference, and “CCEM-K6a/K9” of AC/DC voltage transfer difference.

The thin film multi-junction thermal converters with a novel design have been developed at NMIJ/AIST in collaboration with NIKKOHM Co. Ltd. We have introduced a new thermopile pattern to improve the performance of our thin film MJTC.(*IEEE Trans. Instrum. Meas.*, Vol.64, No.6, 2015.) Using these thermal convertes, novel thermal

converter circuits arranged in an 2 by 2 matrix have been fabricated to improve the low-frequency AC-DC transfer differences (*IEEE Trans. Instrum. Meas.* Vol.68, No.6, 2019). Thin-film AC-DC resistor on an AlN substrate with negligible voltage dependence have been fabricated for measuring AC voltages up to 1000 V (*IEEE Trans. Instrum. Meas.* Vol.68, No.6, 2019). Toward next-generation AC/DC current transfer standard, high-current multijunction thermal conveters on Si substrates up to 1 A have been designed and fabricated through the collaborative project with NIST in Gaithersburg. The results were presented at NCSLI/CPEM2020 and a joint paper has been accepted (*IEEE Trans. Instrum. Meas.* Vol.70, pp. 1-7, 2021).

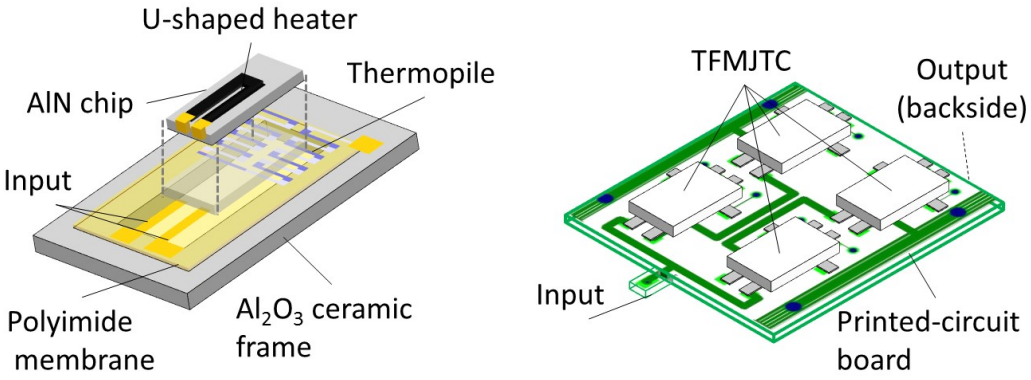

Fig. 6

Toward quantum AC voltage standards, a differential sampling measurement system using an AC-programmable Josephson voltage standard (AC-PJVS) system has been developed (*Meas. Sci. Technol.* 31, 065010 (2020)). To extend the voltage range of the system, we have combined an two-stage inductive voltage divider and an 10 V AC-programmable Josephson voltage standard chip.

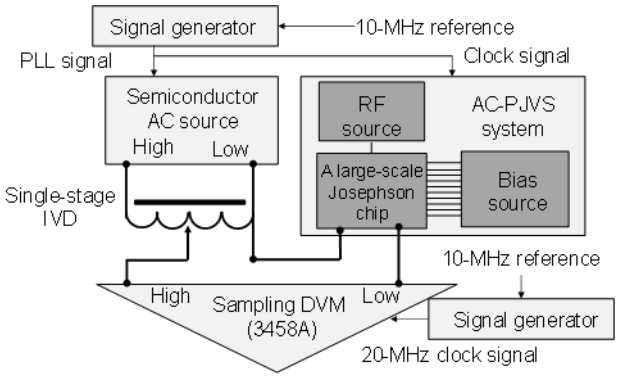

Fig. 7

Toward a waste-heat recovery with thermoelectric conversion, we have developed

advanced metrology techniques and apparatus using a precise ac and dc electrical measurement technique. In particular, the Seebeck coefficient is an essential indicator of the conversion efficiency and the most widely measured property specific to these materials. So far, we have developed a method to precisely measure Thomson effect to determine the absolute Seebeck coefficient of platinum reference material (*IEEE Trans. Instrum. Meas.* Vol.64, No.6, 2015, *AIP Advances* 9, 65312, 2019, *Appl. Phys. Lett.* 117, 063903 (2020), *selected as a Featured Article*). We have also precisely measured the absolute Seebeck coefficient of the fine Pt sample at low temperature below 100 K using a high-*T*c superconductor as a reference (*Rev. Sci. Instrum.* 91, 014903 (2020)). (Contact: Yasutaka Amagai, y-amagai@aist.go.jp, Kenjiro Okawa, okawa.k@aist.go.jp).

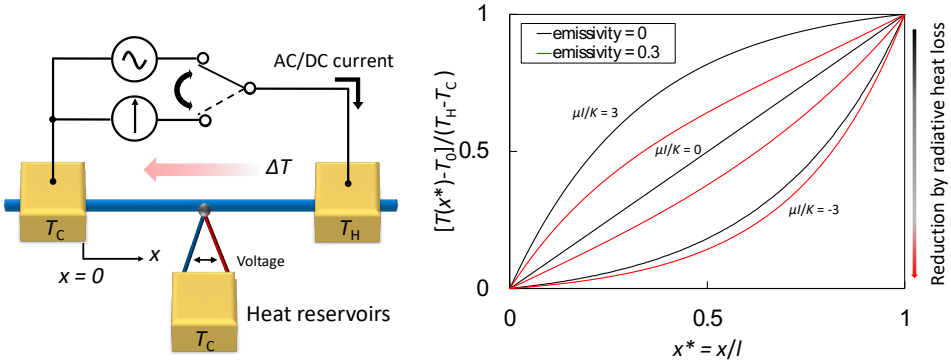

Fig. 8

6. Power (NMIJ)

6.1. Power at NMIJ (harmonics, etc)

We had previously proposed a wideband phase measurement system based on the three-voltmeter method by using a normal thermal voltage converter (TVC) for measuring the differential AC voltage between two AC voltage signals. Several problems were recorded in our previous system, especially for operations in the wideband frequency range. We have investigated their causes and proposed a few solutions. To overcome these problems, we have proposed an additive calibration for the voltmeters by switching the TVC from the differential input mode into a reversible single-ended input mode. The large error peak problem at higher frequencies has been addressed. We compared our proposed system to the new commercial phase standards up to 1 MHz and confirmed the effectiveness of the additive calibration by using the TVC for multiple purposes. The work was presented at CPEM 2020 and will be published (*IEEE Trans. Instrum. Meas.*). (Contact: Tatsuji Yamada, yamada.79@aist.go.jp)

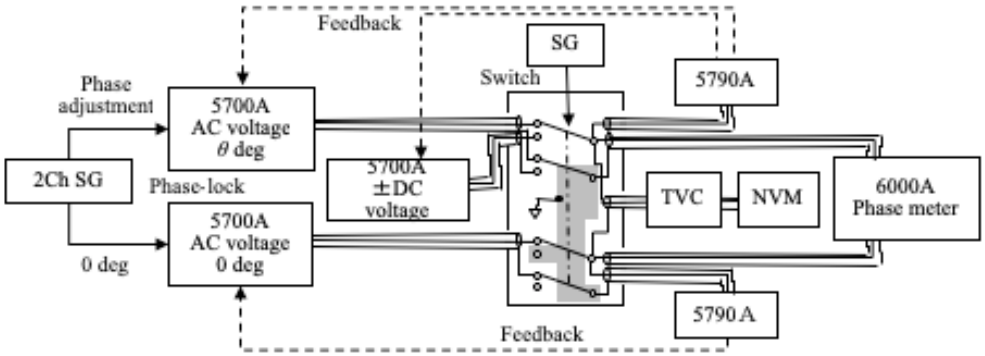

The 3VM-based phase difference measurement system.

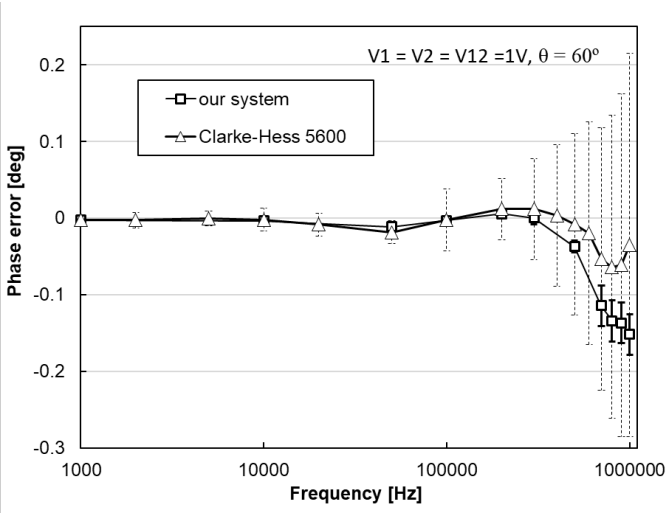

Fig. 9

6.2. Power at JEMIC (mains)

JEMIC has provided the primary active/reactive power/energy standards for the power frequencies in the voltage range from 50 V to 120 V and in the current range from 2.5 A to 50 A. The standard individually measures voltage U and current I with two precise voltmeters and a shunt resistor, and phase θ with a precise digital phase meter. After these measurements, the active and reactive powers are calculated by UI cosθ and UI sinθ, respectively. The representative expanded uncertainties under conditions of 100 V and 5 A are 22 μW/VA (power factor 1) and 10 μW/VA (power factor 0). In 2020, we calibrated approximately 10 power meters and 70 energy meters.

JEMIC has been participating in APMP Key Comparison for APMP.EM-K5.1 of AC power and energy. (Contact: TADOKORO Takuya, t-tadokoro@jemic.go.jp)

7. RF-Power

NMIJ developed a WR-5 waveguide-based calorimeter for the frequency range of 140-220 GHz in collaboration with the National Institute of Information and Communication Technology. Direct comparison calibration was demonstrated for commercially available power meters using the calorimetr as a reference standard. We have begun to provide reference values for the WR-5 band to domestic organizations.(Contact: Yuya Tojima, yuya-tojima@aist.go.jp, Moto Kinoshita, moto-kinoshita@aist.go.jp)

8. RF-Attenuation and Phase Shift

NMIJ has established national standard for RF and microwave attenuation in the frequency range of 100 kHz to 110 GHz, and provides its calibration services mainly with the Japan Calibration Service System (JCSS) scheme. All measurement and calibration systems work based on the intermediate frequency (IF) substitution method using the highly accurate null detection and employing an inductive voltage divider (IVD) as the reference standard. Improvements including measurement system in the 1 kHz to 100 kHz frequency range (Fig.10) are conducting to meet industry requirements regarding electromagnetic compatibility (EMC). (A. Widarta, "Primary standard of attenuation in the frequency range of 1 kHz to 10 MHz," in CPEM Dig., Denver, Co, Aug. 2020, *virtual*).

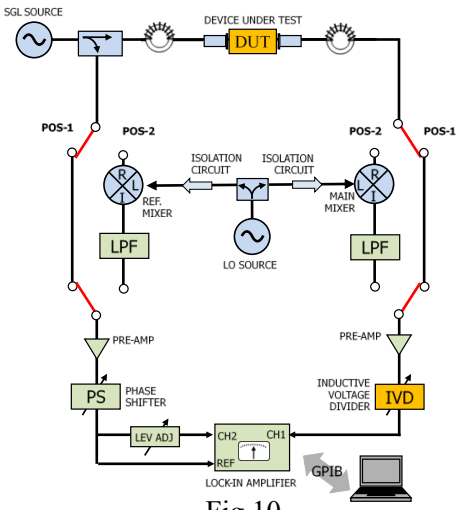

Fig.10

NMIJ established national standard for RF phase shift in the frequency range of 10 MHz to 1 GHz. The expanded uncertainties are 0.029° for DUT with losses up to 20 dB, 0.031° for 40 dB, and 0.056° for 60 dB loss. The frequency range is currently being expanded to 18 GHz. (A. Widarta, "Precision phase shift measurement system in the frequency range of 1-18 GHz, 50th European Microwave Conf., Utrecht, The Netherlands, Jan. 2021).

NMIJ took an initiative to organize a CIPM Key Comparison of attenuation at 18 GHz, 26.5 GHz and 40 GHz using a step attenuator. Measurements of both the first and second round loop were completed on February 2018. It can be said successful, although there were some delays in the delivery of the traveling standards between the participants. Preparation of the Draft A report is started. (Contact: Anton Widarta, anton-widarta@aist.go.jp)

9. RF-Impedance and related measurement technology

NMIJ researched the precision on-wafer measurement techniques over 100 GHz and developed a full-automatic RF probing system establishing high reproducibility of measurements. Balanced type circular disk resonator method has been developped and commarcialized, in addition, the method will be published as an IEC standardization. The method cannot only measure dielectric permittivity but also conductivity at millimeter wave frequency (Fig.10). Furthermore, electromagnetic sensing techniques is also researching for the agriculture products, food and infrastrucre, etc.. In addition, scaning microwave microscopy (SMM) technique are researching and NMIJ originally developed matching circuit to establish high sensitivity and low signal-to-noise ratio. Recently, NMIJ demonstrated percoemance comparison for three SMM system.

NMIJ as a pilot laboratory is managing the CCEM key comparison (CCEM.RF-K5c.CL: S-parameter for PC3.5 in the range from 50 MHz to 33 GHz), the APMP supplemental comparison (APMP.EM.RF-S5.CL: Dimensionally-derived characteristic impedance for PC7, PC2.4 and PC1.85) and the pilot study for material characterization. (Contact: Ryoko. Kishikawa, ryoko-kishikawa@aist.go.jp, Yuto Kato, y-katou@aist.go.jp, Masahiro Horibe, masahiro-horibe@aist.go.jp)

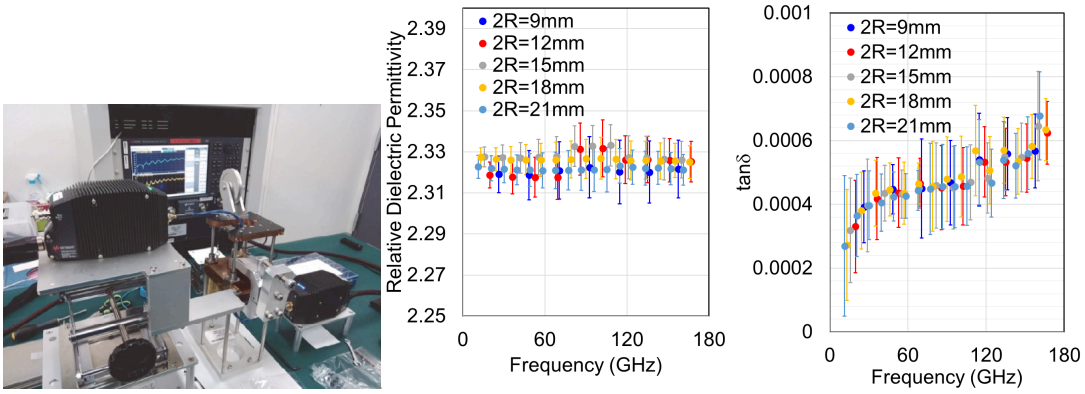

Fig. 11 Balanced type circular disk resonator at millimeterwave frequency

10. Antennas, electric field, and magnetic field

A calibration service for the free-space antenna factor on loop antenna is maintained in the frequency range of 20 Hz to 30 MHz. The expanded uncertainty of the magnetic antenna factor was improved to be from 0.4 dB to 0.7 dB in the frequency range from 9 kHz to 30 MHz in December 2019.

AC Magnetic field sensor calibration service is maintained in a range of 1 uT to 150 uT from 50 Hz to 100 kHz. The realizable field strength depends on frequency points.

(Contact: Masanori Ishii, masanori-ishii@aist.go.jp)

Calibration of the dipole antenna factor above a ground plane from 30 MHz to 1 GHz with the specific conditions (with horizontal polarization and at 2.0 m from the ground plane surface) is available. Since EMC (electromagnetic compatibility) measurements are ordinarily carried out in free space above 1 GHz, the dipole antenna factor from 1 GHz to 2 GHz is calibrated in an anechoic chamber. The free space dipole factor is a traceability source of the E-field strength. (Contact: Takehiro Morioka, t-morioka@aist.go.jp)

The free space antenna factor calibration service for broadband antenna for Biconical antenna (30 MHz to 300 MHz), Log periodic dipole array antenna (300 MHz to 1000 MHz) and Super broadband antenna (30 MHz to 1000 MHz) are being performed using our original three antenna calibration method.
(Contact: Sayaka Matsukawa, sayaka-matsukawa@aist.go.jp)

Calibration services for the gains of standard horn antennas are being performed from 18 GHz to 26.5 GHz using the extrapolation method. An antenna gain calibration service and antenna factor calibration service for ridged guide broadband horn antenna (1 GHz to 6 GHz) is available. (Contact: Yuanfeng She, yuanfeng.she@aist.go.jp)

An antenna gain calibration service for millimeter-wave standard gain horn antenna are being performed form 50 GHz to 75 GHz and 75 GHz to 110 GHz using a time-domain processing and extrapolation technique. Standard gain horn antenna calibration service for 220 GHz to 330 GHz has been started from March 2020. The expanded uncertainty of antenna gain was estimated to between 0.34 dB to 0.5 dB.

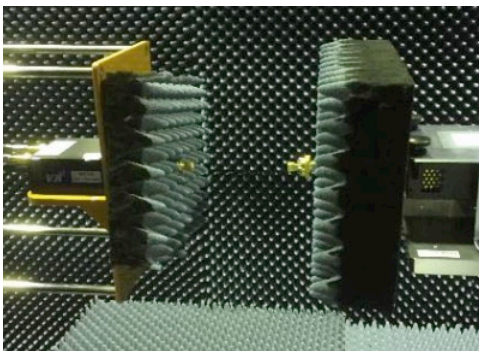

Fig. 12 Antenna gain calibration system

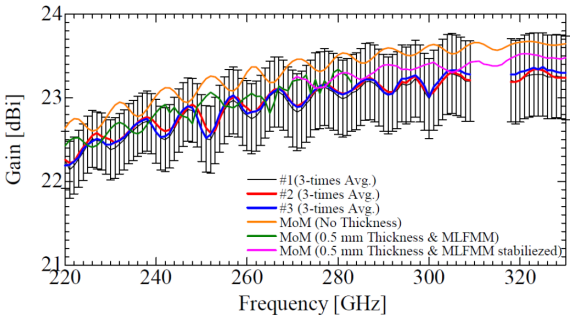

Fig. 13 Estimated antenna gain that compare

RCS calibration service for cylindrical metal reflector and square metal plate in W-band has been started from March 2019 . The expanded uncertainty of RCS for cylindrical metal reflector in W-band was estimated to between 1.1 to 1.6 dB. The expanded uncertainty of RCS for square metal plate reflector in W-band was estimated to between 1.4 dB to 2.1 dB. (Contact: Michitaka Ameya, m.ameya@aist.go.jp)

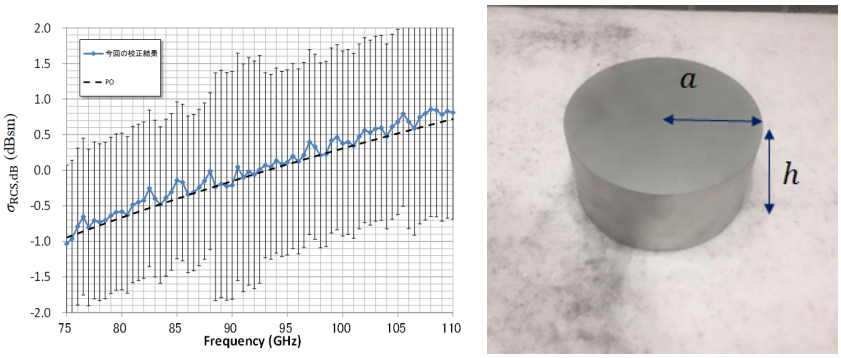

Fig. 14 RCS calibration results in W-band and an example of a cylindrical reflector

The E-field transfer probe calibration from 20 MHz to 4 GHz in a G-TEM cell is available. The E-field transfer probe calibration from 3.8 to 6 GHz in anechoic chamber is available. The correction factor of a probe under calibration is provided when the probe output is 10 V/m and 20 V/m. An optical E-field probe is employed as an E-field transfer probe and the E-field level in the G-TEM cell up to 4 GHz is then calibrated for the ordinary field probe calibration. Three appropriate methods depending on the measurement frequency are employed for the standard E-field generation in calibrating the response of the optical probe. A TEM cell is employed as a standard E-field generator at low frequencies, and the E-field level from 0.8 GHz to 2.2 GHz is calibrated by using the free space dipole antenna factor in the anechoic chamber. Antenna gain is used for the standard field generation in the anechoic chamber from 2 GHz to 6 GHz. (Contact: Takehiro Morioka, t-morioka@aist.go.jp, Michitaka Ameya, m-ameya@aist.go.jp)

11. Terahertz Metrology

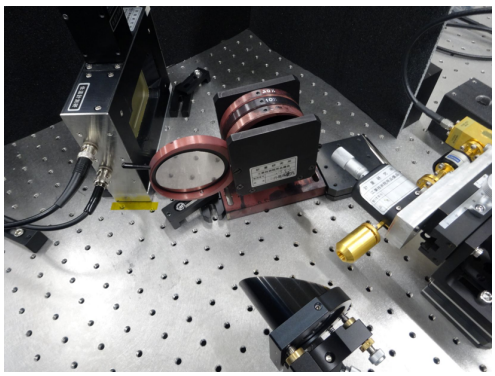

Fig. 15 Photograph of the THz attenuation calibration system for free-space beams.

NMIJ developed a method for measuring terahertz (THz) attenuation for free-space beams. It employs a photo-acoustic detector to compare THz attenuation to audio-frequency (AF) attenuation. The AF attenuation is directly calibrated by an inductive voltage divider as a reference standard. Using a metalized-film attenuator, we have demonstrated attenuation measurements up to 20 dB for 0.11 THz collimated beams. (Contact: Hitoshi Iida, h-iida@aist.go.jp, Moto Kinoshita, moto-kinoshita@aist.go.jp)

12. Material Characterization

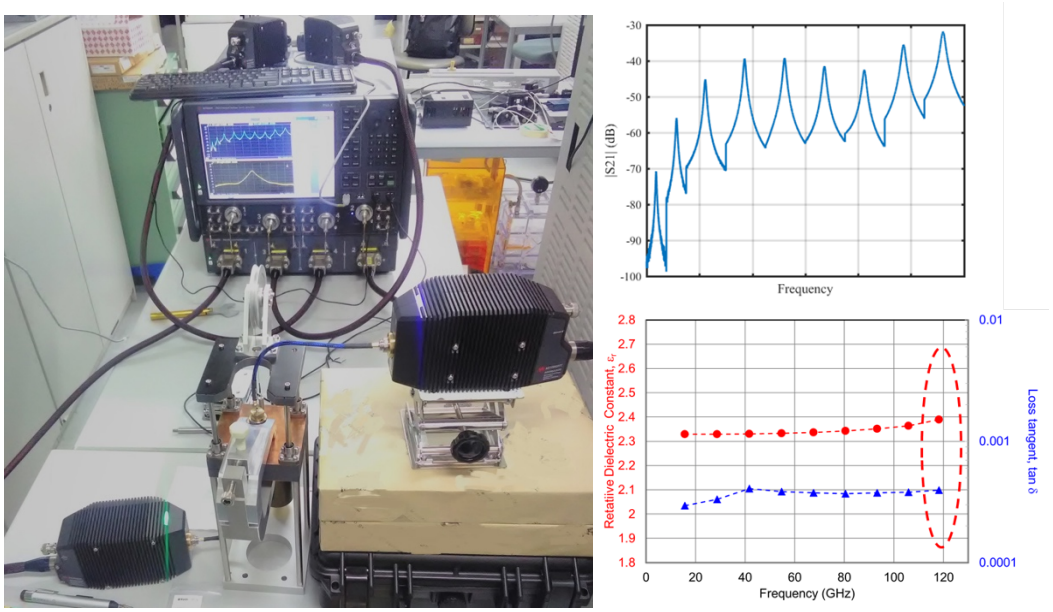

Fig. 16 Photographs of Balanced-type circular-disk resonator(BCDR) and Measurement Results of cyclic olefin polymers (COP) up to 120 GHz

NMIJ is researching and develops material characterization, i.e. dielectric permittivity measurements, at the millimeterwave frequency. NMIJ developed the Balanced-type circular-disk resonator(BCDR) and analytical sofware for dielectroic permittivity of low loss materials. Measurement can be perfformed in broad band frequency and up to 120

GHz (Fig. 19). The method is now being standardized in the IEC standard, then the system has been provided by the measurement instrument company.

Furthermore, NMIJ as a pilot laboratory manages the Pilot study for dielectric permittivity measurement proposed by NIST as a former pilot laboratory in it. (Contact: Yuto Kato, y-katou@aist.go.jp, Masahiro Horibe, masahiro-horibe@aist.go.jp)